



Cite this: *Phys. Chem. Chem. Phys.*,
2016, 18, 14182

Received 20th January 2016,
Accepted 2nd May 2016

DOI: 10.1039/c6cp00420b

www.rsc.org/pccp

Interaction of BODIPY dyes with bovine serum albumin: a case study on the aggregation of a click-BODIPY dye†

Laramie P. Jameson, Nicholas W. Smith, Onofrio Annunziata and Sergei V. Dzyuba*

The fluorescence of BODIPY and click-BODIPY dyes was found to substantially increase in the presence of bovine serum albumin (BSA). BSA acted as a solubilizer for dye aggregates, in addition to being a conventional binding scaffold for the click-BODIPY dyes, indicating that disaggregation of fluorophores should be considered when evaluating dye–protein interactions.

BODIPY dyes are among the most useful and versatile small molecule fluorescent probes, and a wide range of applications has been attributed to the dyes' high thermal and chemical stabilities, high quantum yields, extinction coefficients, as well as tunable spectroscopic properties.^{1–3} In regard to biomolecular processes, BODIPY dyes have been primarily used to label ligands to address ligand–receptor interactions.^{4,5} Recently, several reports suggested that BODIPY dyes could interact directly with a variety of proteins and peptide assemblies, acting as fluorescence-based sensors.^{6,7}

Fluorophore–albumin interactions are of interest, since serum albumins are the major small molecule-binding proteins, which are considered suitable models for various *in vitro* studies on ligand–protein interactions.⁸ In addition, due to its size and collection of binding sites, bovine serum albumin (BSA) could be viewed as a viable model for non-specific binding. Although a number of fluorophores have been shown to bind to albumins, only a few BODIPY dyes have been investigated.^{9–13} Notably, a BODIPY dye was identified (out of a library of 137 dyes) that exhibited *ca.* 200-fold emission enhancement in the presence of BSA, while exhibiting high specificity towards BSA over serum albumins from other species (human, porcine, rat, and sheep).^{11,12} Significantly, specifically substituted BODIPY-based fluorescent probes were shown to be viable sensors of protein hydrophobicity.¹⁴ Furthermore, several common BODIPY dyes, including a water-soluble derivative, were recently suggested to interact with albumins¹⁵ as was evidenced by an increase in the emission intensity.

We previously demonstrated that the incorporation of a triazole moiety on the BODIPY dye scaffold afforded probes that had a significant affinity towards soluble oligomers of amyloid peptides,¹⁶ thus illustrating the possibility for click-BODIPY dyes to act as biosensors.

Here, in order to expand on the utility of BODIPY dyes, we examined the interactions between triazole-containing BODIPY dyes, so-called click-BODIPY dyes, (Fig. 1) and BSA. The incorporation of the triazole group onto the BODIPY scaffold was accomplished in a straightforward manner using an alkyne-containing BODIPY scaffold (ESI†). Dye 2 has a triazole moiety, and the presence of the methyl group, rather than the benzyl group, assures that dye 2 is less hydrophobic than dye 3.

During the initial screening, the fluorescence of dyes 1, 2, and 3 was measured in the presence of a fixed amount of BSA (39.2 μ M) and a notable enhancement in the fluorescence of the dyes in the presence of BSA was observed (Fig. 2).

At the highest experimental dye concentration (1 μ M), krypto-BODIPY dye 1 exhibited a *ca.* 20-fold increase in its fluorescence

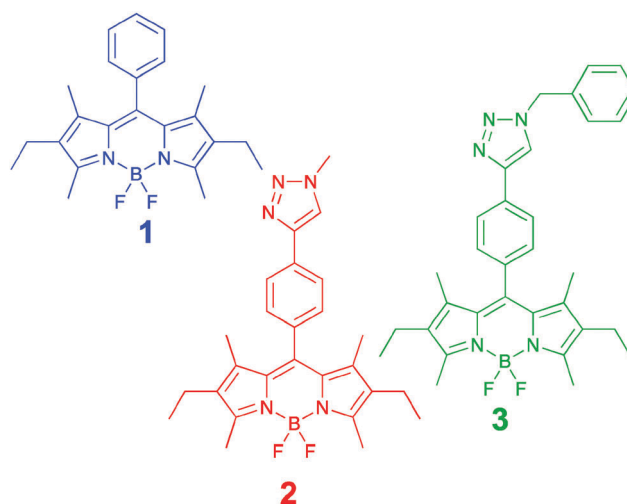


Fig. 1 Structures of krypto-BODIPY (1) and click-BODIPY (2 and 3) dyes.

Department of Chemistry and Biochemistry, Texas Christian University, Fort Worth, TX 76129, USA. E-mail: s.dzyuba@tcu.edu

† Electronic supplementary information (ESI) available: Synthesis and characterization of BODIPY dyes; details on the fluorescent experiments and sample preparations. See DOI: 10.1039/c6cp00420b

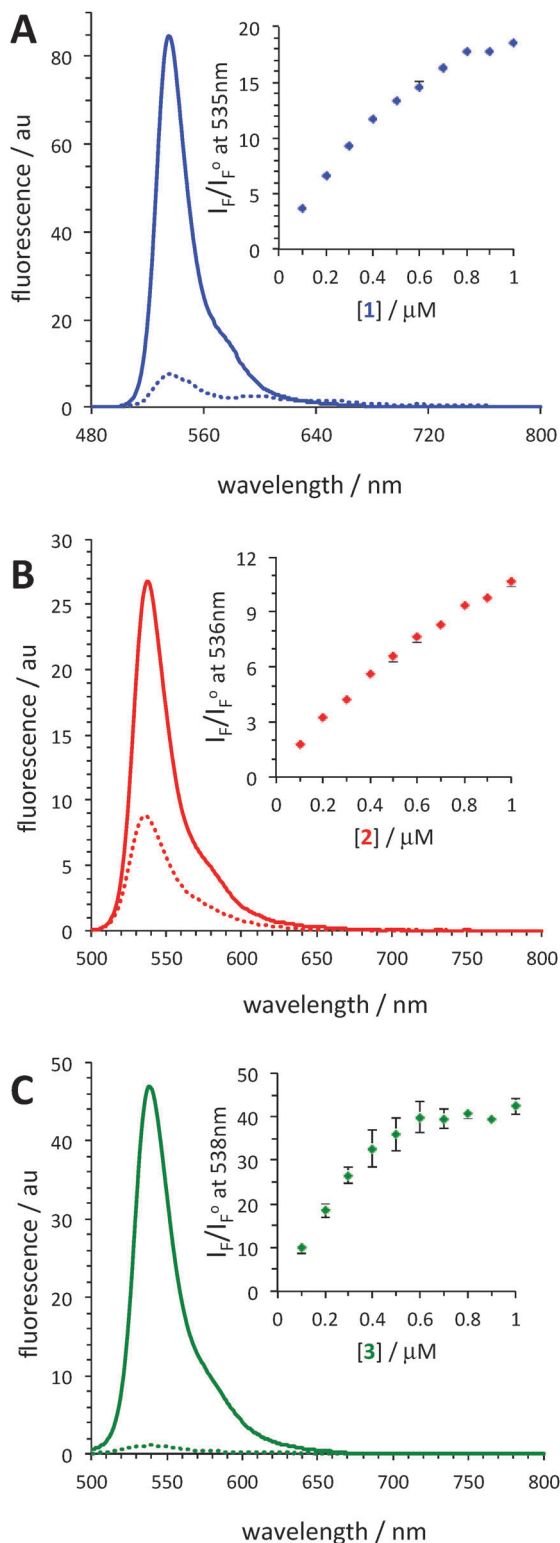


Fig. 2 Representative fluorescence spectra of BODIPY dyes (0.5 μM) **1** (A), **2** (B), and **3** (C) in the presence (solid line) and absence (dotted line) of BSA (39.2 μM). $\lambda_{\text{ex}} = 475 \text{ nm}$. Buffer: 10 mM TRIS (0.1 M NaCl, pH 7.4). Insets: Fluorescence enhancement as a function of dye concentration; I_F – fluorescence in the presence of BSA, I_F^0 – fluorescence in the absence of BSA. The data are the average of 2–3 measurements \pm SD.

intensity in the presence of BSA, while the introduction of the methyl-triazole moiety, dye **2**, resulted in only a 10-fold increase. Remarkably, in the presence of BSA, dye **3** exhibited a significantly larger enhancement, *ca.* 40-fold. Notably, the fluorescence enhancement of dye **3** compared to that of dyes **1** and **2** could be viewed as even more remarkable at lower dye concentrations (*e.g.*, 0.2 μM), since the fluorescence of dye **3** saturated at dye concentrations greater than 0.5 μM . It should also be pointed out that the absorption spectra of the dyes were not drastically different in the absence and presence of BSA (Fig. S1–S6, ESI†).

Furthermore, the fluorescence intensity of dye **3**, in the presence of BSA, was found to increase with time, t , towards its asymptotic equilibrium value. This was likely related to the kinetics of protein–dye association and the corresponding desolvation effects of the dye and its aggregates. This behavior was not observed in the case of the other two dyes, *i.e.*, no time-dependent increase in the emission was observed upon addition of dyes **1** and **2** to the solution of BSA. For dye **3**, the fluorescence intensity at equilibrium, $I_F(\infty)$ was obtained by fitting the time-dependent fluorescence, $i_F(t)$, to the first-order kinetic expression $I_F(\infty)[1 - a \exp(-bt)]$, where $I_F(\infty)$, a , and b are fitting parameters. A representative profile is shown in Fig. 3.

The aforementioned observations may be related to the presence of the benzyl group on dye **3**, which increases the hydrophobicity of the dye, and as such the dye's interaction with hydrophobic binding pockets of the protein should be favored. However, the saturation of the fluorescence signal was taking place at dye concentrations of *ca.* 0.5 μM (Fig. 2C). In order to gain insight into the BODIPY–BSA interactions, we carried out more detailed titration experiments at dye concentrations that were below the saturation point using fluorescence spectroscopy.

The titration conditions were chosen such that the total concentration of protein P (C_P) was large enough when compared

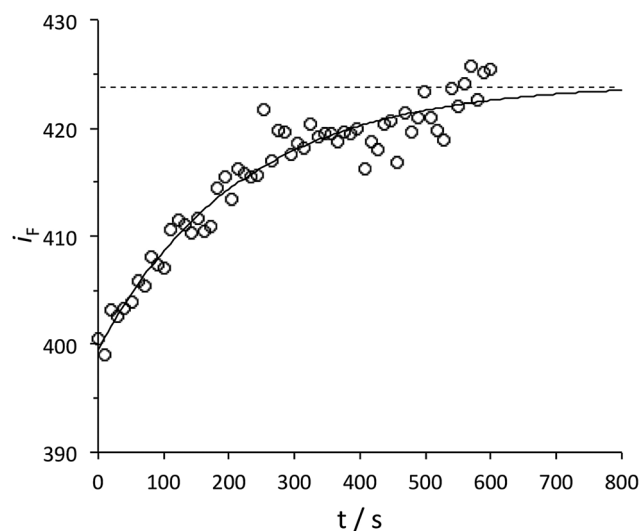


Fig. 3 Experimental fluorescence intensity of dye **3**, i_F , as a function of time, t , at $C_D = 0.3 \mu\text{M}$ and $C_P = 8.7 \mu\text{M}$ (open circles); $\lambda_{\text{ex}} = 530 \text{ nm}$; $\lambda_{\text{em}} = 538 \text{ nm}$; buffer: 10 mM TRIS (0.1 M NaCl, pH 7.4). The solid curve is a fit through the data using $I_F(\infty)[1 - a \exp(-bt)]$. The dashed horizontal line indicates the obtained value of $I_F(\infty)$.



to the total concentration of the dye D (C_D). Thus, it could be assumed that only a 1 : 1 complex of protein–dye (PD), would form appreciably, irrespective of the number of binding sites of BSA. This reversible interaction could be represented as $P + D \rightleftharpoons PD$, with the following mass action law (eqn (1)):

$$K = \frac{[PD]}{[P][D]} \quad (1)$$

where K is the corresponding association constant and $[P]$, $[D]$, and $[PD]$ are the concentrations of the three reaction species at equilibrium, which are linked to the total concentrations by the mass balances: $C_D = [D] + [PD]$ and $C_P = [P] + [PD]$. To determine K , we examined the effect of C_P at a constant C_D on the observed fluorescence enhancement, $F \equiv I_F/I_F^0$, where I_F and I_F^0 are the fluorescence intensities in the presence and in the absence of BSA, respectively. Assuming that fluorescence intensity is directly proportional to fluorophore concentration, it follows:

$$F = 1 + (R - 1)\alpha \quad (2)$$

where R is the fluorescence ratio of bound to free dye (fluorescence gain) and α is the fraction of bound dye (defined as $\alpha \equiv [PD]/C_D$). Eqn (3) is obtained from the mass balances and eqn (1):

$$\alpha = \frac{1 + KC_P + KC_D - \sqrt{(1 + KC_P - KC_D)^2 + 4KC_D}}{2KC_D} \quad (3)$$

The titrations were performed by varying the protein concentration C_P while keeping the dye concentration C_D constant at 0.20 μM . The results were subsequently fitted using eqn (2) and (3), and the results are shown in Fig. 4 and Table 1. The binding constants for all dyes were very similar, and therefore a drastic increase (a 34-fold increase of the fluorescence of the dye 3 as compared to dyes 1 and 2, which showed 1.5 and 2.9 fold increases, respectively) could not be explained by a difference in the binding affinities.

The observed saturation in the fluorescence behavior of dye 3 (Fig. 2C) required additional explanation. At 0.5 μM of the dye, the protein was present in a large excess as compared to

Table 1 Binding constants and fluorescent enhancement upon dye binding to BSA^a

Dye	$K/\mu\text{M}^{-1}$	R^b
1	0.34 ± 0.03	2.9 ± 0.1
2	0.29 ± 0.15	1.5 ± 0.1
3	0.12 ± 0.01	34 ± 1

^a Buffer: 10 mM TRIS (0.1 M NaCl, pH 7.4). ^b Fluorescence ratio of bound to free dye.

the dye, and the saturation of a binding site was unlikely. We considered the self-aggregation of dye 3 as a competitor to the protein–dye binding in solution. Furthermore, these aggregates were assumed to have a minor contribution to the overall fluorescence, since typically aggregation-induced quenching of fluorescence is reported for the vast majority of fluorophores.^{17,18}

In regard to the dye–BSA interaction, the dye aggregation could be assessed when fluorescence intensity (expressed as $I_F - I_F^0$, where I_F^0 is the fluorescence intensity of the protein-free system) is plotted as a function of C_D at constant C_P (Fig. 4). At low protein concentrations, $I_F - I_F^0$ reached a plateau as the dye concentration was increased. This plateau decreased as the protein concentration increased. It is important to note that the protein concentration was significantly larger than that of the dye in all cases, which precludes the saturation of the protein's binding sites. In this case, the protein likely acted as a solubilizer for the dye, and thereby reduced the amount of dye aggregates in solution. Such solubilization by BSA could also explain the disappearance of the plateau in the titration experiments at higher protein concentrations (Fig. 5).

In order to quantitatively describe the observed behavior, dye reversible aggregation could be represented as $nD = D_n$, with the following mass action law (eqn (4)):

$$\beta = S_D^{-(n-1)} = \frac{[D_n]}{[D]^n} \quad (4)$$

where, for simplicity, it is assumed that only one monodisperse mesoscopic aggregate, D_n , is formed with aggregation number n , and β is the corresponding association constant. When $n \gg 1$, the aggregate could be treated as a separate phase, and S_D in eqn (4) represents the solubility of monomeric D with respect to the aggregates in water.¹⁹ For a given n , either β or S_D could be equivalently utilized to characterize aggregation thermodynamics. In our case, we choose to use S_D due to its more direct graphical identification. Since the contribution of dye aggregates to fluorescence was neglected, the difference in intensity, $I_F - I_F^0$ could be described as follows:

$$I_F - I_F^0 = k_F(R[P] + [D] - [D]_0) \quad (5)$$

where k_F is the proportionality constant describing the effect of free monomeric dye on fluorescence intensity and $R = 34$ (Table 1). At a given C_D , $[D]$ and $[D]_0$ represent the concentrations of free monomeric dye in the presence and absence of BSA, respectively. Note that $([D] - [D]_0)$ is small compared to $R[P]$ in eqn (5). The concentrations $[PD]$, $[D]$, and $[D]_0$ can be related to C_D and C_P by the mass balances:

$$C_D = [D] + K[D]C_P/(1 + K[D]) + nS_D([D]/S_D)^n \quad (6)$$

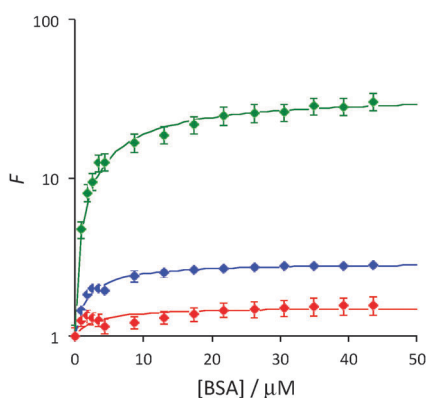


Fig. 4 Experimental fluorescence ratios ($F = I_F/I_F^0$) as a function of protein concentration, C_P , at constant dye concentration, $C_D = 0.20 \mu\text{M}$, for dyes **1** (blue), **2** (red), and **3** (green); $\lambda_{\text{ex}} = 530 \text{ nm}$; $\lambda_{\text{em}} = 538 \text{ nm}$; buffer: 10 mM TRIS (0.1 M NaCl, pH 7.4); the data are the average of 2–3 measurements \pm SD. The solid curves are the theoretical fits through the experimental data, obtained using eqn (4) and (5).



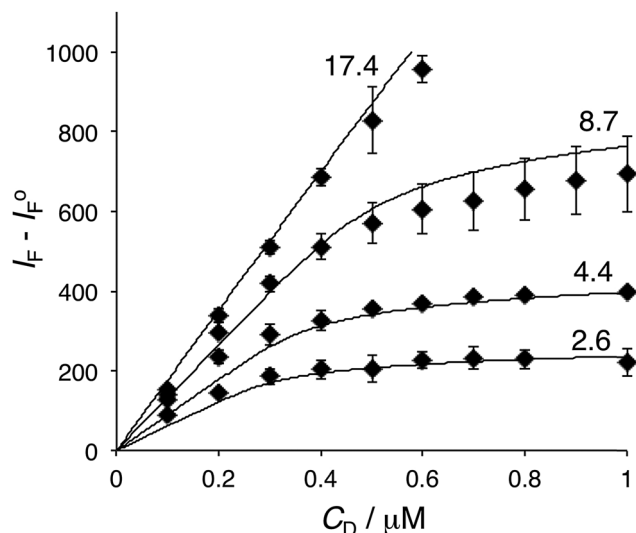


Fig. 5 Experimental fluorescence intensity difference, $I_F - I_F^0$, as a function of dye concentration, C_D at several protein concentrations, C_P (diamonds; the numbers associated with each curve identify the corresponding experimental values of C_P in μM). The data are the average of 2–3 measurements \pm SD). The solid curves represent $I_F - I_F^0$ calculated using eqn (6) and (7) with $K = 0.12 \mu\text{M}^{-1}$, $n = 10$, $S_D = 0.40 \mu\text{M}$, and proportionality constant, $k_F = 75 \mu\text{M}^{-1}$. Conditions: $\lambda_{\text{ex}} = 530 \text{ nm}$, $\lambda_{\text{em}} = 538 \text{ nm}$; buffer: 10 mM TRIS (0.1 M NaCl, pH 7.4).

$$C_D = [D]_0 + nS_D([D]_0/S_D)^n \quad (7)$$

eqn (6) and (7) could be used to numerically calculate $[PD]$, $[D]$, and $[D]_0$ as a function of C_D at constant C_P provided that K , S_D , and n are known. The corresponding $I_F - I_F^0$ curves could then be computed using eqn (5), assuming that k_F is also known. Note that k_F is related to the initial slope of the $I_F - I_F^0$ curves (Fig. 3), S_D to the dye concentration at which the $I_F - I_F^0$ reaches a plateau, and n to the change in the $I_F - I_F^0$ slope as the plateau is approached. To compute $I_F - I_F^0$ curves at the four experimental C_P values (Fig. 3), we used $K = 0.12 \mu\text{M}^{-1}$ from Table 1 and set $k_F = 75 \mu\text{M}^{-1}$, $n = 10$, and $S_D = 0.40 \mu\text{M}$. These curves (Fig. 4) were in a satisfactory agreement with our experimental results. It is also important to mention that the experimental value of $S_D = 0.20 \mu\text{M}$ used to determine K was well below the “solubility” value, S_D .

Conclusions

The interaction of several BODIPY dyes with BSA has been investigated using fluorescence spectroscopy. In the presence of BSA, krypto-BODIPY and click-BODIPY dyes exhibited a notable increase in their fluorescence intensities. In the case of the benzyl-triazole-containing BODIPY dye 3, a drastic increase in the fluorescence intensity was noted, yet the binding affinities for all three dyes towards BSA were found to be virtually the same. The fluorescence enhancement in this particular case demonstrates that BSA could play a dual role: (a) disaggregate the dye's aggregates and (b) subsequently bind monomeric BODIPY 3. Notably, a similar disaggregation phenomenon was also reported for aza-BODIPY dyes.²⁰ Our results suggest that, at least

in some cases, the fluorescence enhancement upon a dye–protein interaction might not be exclusively attributed to the binding event. Potentially the disaggregation of click-BODIPY dyes could be used as a detection event²¹ as well as a sensor for the hydrophobic surfaces of the proteins.¹⁴

Acknowledgements

The project was partially supported by NIH R15AG038977 from the National Institute On Aging (to SVD) and ACS-PRF 47244-G4 (to OA).

Notes and references

- 1 G. Ulrich, R. Ziessel and A. Harriman, *Angew. Chem., Int. Ed.*, 2008, **47**, 1184–1201.
- 2 N. Boens, V. Leen and W. Dehaen, *Chem. Soc. Rev.*, 2012, **41**, 1130–1172.
- 3 A. Loudet and K. Burgess, *Chem. Rev.*, 2007, **107**, 4891–4932.
- 4 T. Kowada, H. Maeda and K. Kikuchi, *Chem. Soc. Rev.*, 2015, **44**, 4953–4972.
- 5 A. Kamkaew, S. H. Lim, H. B. Lee, L. V. Kiew, L. Y. Chung and K. Burgess, *Chem. Soc. Rev.*, 2013, **42**, 77–88.
- 6 H. Sunahara, Y. Urano, J. Kojima and T. Nagano, *J. Am. Chem. Soc.*, 2007, **129**, 5597–5604.
- 7 S.-I. Niu, C. Ulrich, P.-Y. Renard, A. Romieu and R. Ziessel, *Chem. – Eur. J.*, 2012, **18**, 7229–7242.
- 8 C. Bertucci and E. Domenici, *Curr. Med. Chem.*, 2002, **9**, 1463–1481.
- 9 J.-S. Lee, H. K. Kim, S. Feng, M. Vendrell and Y.-T. Chang, *Chem. Commun.*, 2011, **47**, 2339–2341.
- 10 T. Komatsu, D. Oushiki, A. Takeda, M. Miyamura, T. Ueno, T. Terai, K. Hanaoka, Y. Urano, T. Mineno and T. Nagano, *Chem. Commun.*, 2011, **47**, 10055–10057.
- 11 M. Vendrell, G. G. Krishna, K. K. Ghosh, D. Zhai, J.-S. Lee, Q. Zhu, Y. H. Yau, S. G. Shochat, H. Kim, J. Chung and Y.-T. Chang, *Chem. Commun.*, 2011, **47**, 8424–8426.
- 12 J. C. Er, M. K. Tang, C. G. Chia, H. Liew, M. Vendrell and Y.-T. Chang, *Chem. Sci.*, 2013, **4**, 2168–2176.
- 13 X. Duan, P. Li, P. Li, T. Xie, F. Yu and B. Tang, *Dyes Pigm.*, 2011, **89**, 217–222.
- 14 N. Dorh, S. Zhu, K. B. Dhungana, R. Pati, F.-T. Luo, H. Liu and A. Tiwari, *Sci. Rep.*, 2015, **5**, 18337, DOI: 10.1038/srep18337.
- 15 Yu. S. Marfin, E. L. Aleksakhina, D. A. Merkushev and E. V. Rumyantsev, *J. Fluoresc.*, 2016, **26**, 255–261.
- 16 N. W. Smith, A. Alonso, C. M. Brown and S. V. Dzyuba, *Biochem. Biophys. Res. Commun.*, 2010, **391**, 1455–1458.
- 17 J. Liang, B. Z. Tang and B. Liu, *Chem. Soc. Rev.*, 2015, **44**, 2798–2811.
- 18 J. R. Lakowicz, *Principles of Fluorescence Spectroscopy*, Springer, 2009.
- 19 R. Nagarajan, in *Surfactant science and technology: retrospect and prospects*, ed. L. Romsted, 2014, pp. 3–52.
- 20 X.-X. Zhang, Z. Wang, X. Yue, Y. Ma, D. O. Kiesewetter and X. Chen, *Mol. Pharmaceutics*, 2010, **10**, 1910–1917.
- 21 D. Zhai, W. Xu, L. Zhang and Y.-T. Chang, *Chem. Soc. Rev.*, 2014, **43**, 2402–2411.

